Towards the Development of CO$_2$ Separation Membranes

Gerard Caneba*, Michael Renier, and Brian Ott

Department of Chemical Engineering and
Center for Environmentally Benign Functional Materials (CEBFM)
Michigan Technological University, Houghton, MI 49931
*Email: caneba@mtu.edu

Abstract

This work pertains to current results in the development of CO$_2$ separation membranes from flue gas streams typically found in coal-fired power plants. A versatile free-radical-based polymerization method is employed for the development of a multifunctional block copolymer that has good affinity to CO$_2$, is processable into and applicable as gas separation polymer membranes. In order to validate the resulting materials, thin slabs of the polymer were melt-processed, and then sorbed with CO$_2$ and N$_2$ in a pressure cell. When the pressure is released, foaming tendencies at the outer regions of the samples were observed. A quantitative model involving measurements of unfoamed regions is used to correlate with permeability ratios as well as CO$_2$-polymer mutual diffusivities. One particular optimized material, called RB1-215, is shown to possess a good CO$_2$ relative permeability to N2. Thus, the experimental methodology has been shown to possibly be able to develop the next generation of CO$_2$ separation polymer membranes for carbon sequestration applications.

Keywords
Carbon sequestration, polymer membranes, CO$_2$ separation, flue gases, FRRPP process

1. INTRODUCTION

The separation of CO$_2$ from flue gases in coal power plants has been known to be an attractive method of sequestering potential global warming/climate change gases. In this regard, the use of membrane separation of CO$_2$ is attractive because of energy savings that can potentially be realized. For example, conventional methods rely on cryogenic conditions in order to absorb the CO$_2$ even with the use of favorable fluids, such as ammonia, amines, glycols, etc. The problem of CO$_2$ sequestration from flue gases reduces to its separation from N$_2$ gas, because other components are either minor, easily

removable, or can be included with the CO_2-rich product stream. Thus, good CO_2 separation factor relative to N_2 in polymer membranes translates to a viable CO_2 sequestration operation.

Gas membrane separation in this paper involves the solution-diffusion mechanism of the penetrant through a polymer film. Penetrant is introduced on one side of the film and the other side is maintained at a lower penetrant concentration. The rate per unit film area at which the penetrant traverses the thickness of the film is related to the diffusivity. Details of the calculation of the diffusivity depend on the type of experiment used.

1.1 Steady-State Experiment

In the steady-state experiment, the film with thickness L has no penetrant at the beginning. At time t=0, the upstream face of the film is exposed to a constant penetrant concentration C_1, while the downstream face is exposed to a lower constant penetrant concentration, C_2. If the system is at steady-state and there is no chemical reaction in the film, the flux F of the penetrant is constant. Fick's first law of diffusion results in

$$F = \frac{D(C_1 - C_2)}{l} \tag{1},$$

where D is the mutual diffusivity.[1] Note that Equation 1 applies to constant diffusivity for a binary system.

For a multicomponent penetrant system, it is customary to apply Equation 1 for each of the penetrant components, provided these components do not interact with one another. Also, it is customary to express the penetrant i concentration in terms of its partial pressure on the corresponding face of the membrane (Henry's Law), such as

$$C_i = S_i p_i \tag{2}.$$

Thus, for a noninteracting multicomponent penetrant system following Equation 2 (Henry's Law) Equation 1 becomes

$$F_i = P_i(p_{i1} - p_{i2}) \tag{3},$$

Where P_i is the permeability of component i. If are comparing relative fluxes of penetrants A (such as CO_2) and B (such as N_2) through the polymer membrane, then the permeability ratio or separation factor between A and B is obtained as

$$\alpha_{AB} = \frac{P_A}{P_B} = \frac{D_A S_A}{D_B S_B}$$

(4).

Values for permeability ratios for CO_2 relative to N_2 are 17 in polysulfones and 6 in PDMS, and these membranes have N_2 permeabilities of 0.5-5 L(STP)/min-m^2-atm and 5-50 L(STP)/min-m^2-atm, respectively.[2] Thus, the task of membrane design is to increase both selectivity and flux of CO_2 compared to N_2 at various prevailing temperatures and pressures.

1.2 Concentration-Distance Measurements

The idea behind this approach is the measurement of the concentration profile of the penetrant, with subsequent calculation of the diffusivity. Methods of measurement of penetrant concentration include the use of various means of establishing contrast. A simple way is to use differences in light intensities if the penetrant includes a dye in it. Another method is based on refractive index differences with penetrant concentration. In the interference technique,[3,4] Fabry-Perot fringes corresponding to refractive index contours are obtained when viewing the polymer perpendicular to the diffusion direction through semi-silvered glass plates with about 10 % light transmission. If the refractive index is known as a function of concentration in the monotonic sense, then concentration-distance curves can be easily obtained from the fringe pattern. If the refractive index has a maximum with concentration, it is still possible to calculate the concentration-distance curve with some difficulty. Another way of obtaining the refractive index profile is through the Lamm scale method developed by Hutcheon and coworkers as a microtechnique.[5] They used a 1-m focal length at unit magnification to record the "distorted" scale photographically. The scale displacements on the plate are related to the refractive index gradient.

Other detection methods for the concentration profile that have been used in the past include the use of radiotracers.[6-9]

The simplest way of using concentration profile measurements is to cut the film into parallel strips along the direction of diffusion after steady state is reached. From concentration measurements of the strips of swollen polymer and the flux of penetrant, Equation 1 can be used to calculate the diffusivity. This approach was first used by Gillespie and Williams to obtain the diffusivity of water in cellulose acetate.[10]

From the measured concentration profile of the unsteady-state system, the error-curve method has also been introduced to determine constant diffuvities.[11] For calculation of

concentration-dependent diffusivities, the Matano method has been used to determine diffusivities of the whole concentration range of the polymer and penetrant.[12]

It is also possible to estimate the penetration distance of a penetrant by subsequently dropping the penetrant pressure to cause it to form a foam in the polymer. An examination of the foamed front provides an idea of the penetration depth and thus, the penetrant diffusivity within the polymer. This penetration depth is also related to the solubility of the penetrant, since a threshold amount of solubility is needed for a foam to form within the polymer. Details can be quantitatively resolved by considering the problem as that of a semi-infinite polymer medium for the penetrant. Since it takes about 6 wt % of blowing agent to form a foam, then the lowest penetrant concentration of the foam layer can be considered to be at 6 wt %.

2. EXPERIMENTAL

2.1 Polymer Design

Among all the polymerization methods, only the free-radical-based mechanism offers a robust technique in implementing the formation of block copolymer materials with the widest variety of monomer types. The reason is that reactive sites (acid, base, hydrogen bonds, ions) from some of the more useful monomers normally interfere with the clean formation of the polymer chain. Whereas, free radicals do not normally interact with other reactive groups in various monomers and polymer segments. Also, solvents used in the polymerization process normally do not interfere with free-radical reactivities, while other polymerization mechanisms can be sensitive to the solvent used. Thus, selection of solvent(s) in a mixture of monomers to impart multifunctionality is very difficult, unless a free-radical-based polymerization mechanism is employed. It should therefore be no surprise that commercially sold polymer membranes are made from premade resins or their modified forms. Even for these materials, they are sold with almost no flexibility in terms of the functionalities of their segments during polymerization; functional flexibility is imparted through functionalization reactions of side groups, which is limited at best.

In this work, a collection of monomers, oligomers, and/or polymers possessing various chemical groups are incorporated within a set of polymer chains that make up the main component of the composition. These functional groups may be naturally present in the raw materials used to produce the multifunctional multipolymeric membranes, or may be purposely or naturally altered by modifying reactions. A subpolymer (equivalent to a number of monomer segments) representation of these chemical functionalities in a portion of the entire polymer is shown in Figure 1, which is depicted by the A,B,C,D,…-

functionalities emanating from various polymer segments within the subpolymers. To form block copolymers, there will be a set of adjacent segments that have the same functional groups.
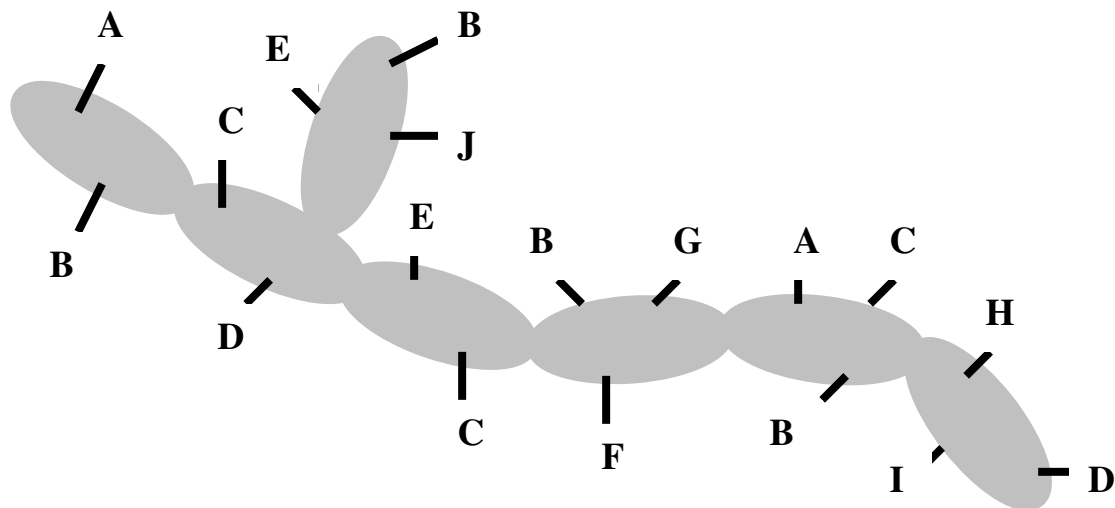

Figure 1. Subpolymer representation of proposed multifunctional multipolymeric membrane materials with various functional groups (A, B, C, D, …)

Table 1. Possible functionalities (A,B,C,D,…) for the above structural representation of the multifunctional multipolymeric membranes. Examples of commercial polymers with various functionality classes as well as their corresponding application features are given.

A,B,C,D,…-Functionality Class	Examples of A,B,C,D,…-Functionality found in Commercial Polymers	Application features of functional groups
Hydroxyl	Poly(vinyl alcohol)	Biodegradability, adhesion to polar surfaces (wood, masonry, cement), colloidal properties
Ketone	Poly(methyl vinyl ketone), Poly(isopropyl vinyl ketone), Ethylene-Carbon Monoxide Copolymers	Carbon dioxide absorption, UV degradability, distinct UV absorbance
Ester	Poly(vinyl acetate), Poly(methyl acrylate), Poly(ethyl acrylate), Poly(methyl methacrylate), poly(butyl acrylate), Ethylene-Vinyl Acetate Copolymers	Good interactions with carbon dioxide, adhesion to polar surfaces and for composition adjustment based on application temperature
Carboxylic acid	Poly(acrylic acid), Poly(methacrylic acid),	Reactivity with metal and

	Ethylene-Acrylic Acid Copolymers, Ethylene-Methacrylic Acid Copolymers	non-metal bases with and without additional functionalities, Water dispersibility, adhesion to metals
Amine	Poly(acrylamide), Poly(isopropyl acrylamide)	Good interactions with carbon dioxide, reactivity with acids with and without additional functionalities, Water dispersibility
Epoxy	Glycidyl methacrylate copolymers	Self-crosslinking, reactivity with amines, isocyanates, alcohols
Aromatic Hydrocarbon	Polystyrene	Source of chromophores, and capability of modification of the aromatic ring (such as sulfonation)
Aliphatic Hydrocarbon	Polyolefins	Affinity to hydrocarbon oils and moisture resistance
Halogens	Poly(vinylidene chloride), poly(vinylidene fluoride), polychlorotrifluoroethylene, polytetrafluoroethylene, Zonyl™ copolymers	Superior strength, chemical, thermal, fire resistances, Zonyl™ copolymers have good carbon dioxide interactions

Note that the above table shows functionality classes that could impart carbon dioxide permeability in the overall polymer.

A two-plus stage reactor procedure is proposed using the design-of-experiment guidelines (DOE) in Table 2 below, using the so-called free-radical retrograde-precipitation polymerization process.[13-14]

The development of an optimized polymer as membrane material for CO_2 separation could first be done through a selection of basic features, such as CO_2 absorption, strength, reactive and/or nonreactive adhesion/crosslinker, and chemical/thermal resistances. In addition, processability aspects have been looked into through low temperature elasticity segments and use of various possible block copolymer architectures, such as diblock and triblock-type of copolymers. A halogenated RB1-215 triblock (A-B-C) material with strength A-group, reactive B-group, and CO_2-interacting C-group was developed.

The development of the RB1-215 material was done through a design-of-experiment approach as shown in the Table 2. Its proposed morphological structure is shown in Figure 3 below.

Table 2. DOE matrix and responses expected from the block copolymer under development.

#	!st Stage		2nd Stage			Arc.	Responses				
	V	C	Z	G	B	D,T	Strength	CO$_2$ Absorption	Chem Resis.	Thermal Resis.	Adh.
1	H	L	L	L	L	D	L	L	TBD	TBD	TBD
2	H	L	L	H	L	D	H	L	TBD	TBD	H
3	H	L	H	H	L	D	TBD	H	TBD	TBD	H
4	H	L	H	L	L	D	TBD	H	TBD	TBD	TBD
5	H	L	L	L	L	T	H	L	TBD	TBD	TBD
6	H	L	L	H	L	T	H	L	TBD	TBD	H
7	H	L	H	H	L	T	H	H	TBD	TBD	H
8	H	L	H	L	L	T	H	TBD	TBD	TBD	TBD

V – for strength
C – comonomer for reaction facilitation/processability of strength monomer (V)
Z – for CO$_2$ absorption
G – for adhesion/crosslinking promoter
B – for low temperature elasticity
D – Diblock-based molecular architecture
T – Triblock-based molecular architecture

First Stage Compositions (based on first stage polymer):
L – 5-15%
H – 50-90%
Second Stage Compositions (based on overall polymer unless otherwise noted):
L – 0-20% (B based on 2nd stage polymer), 10-20% (Z,G)
H – 20-40%

Both high pressure (4,500 psig) metal and low pressure (45 psig) glass stirred-tank reactor systems have been used in this work (Figure 2 below), recipes and conditions were generated using high throughput experimentation methods.
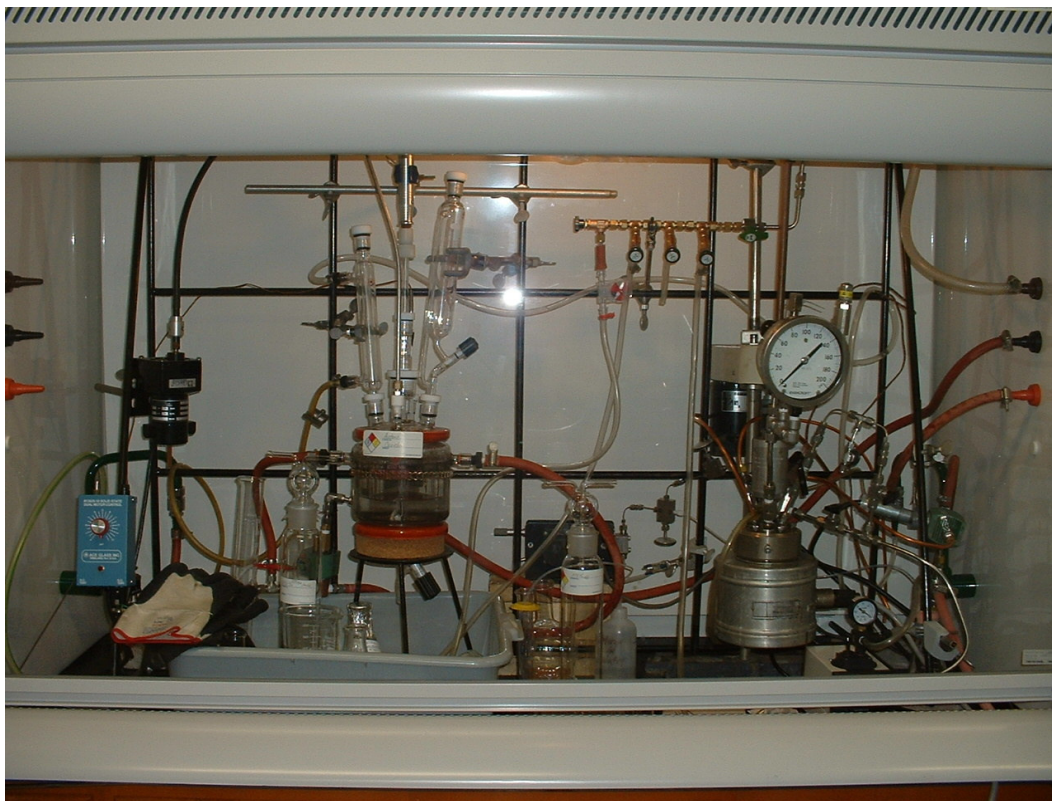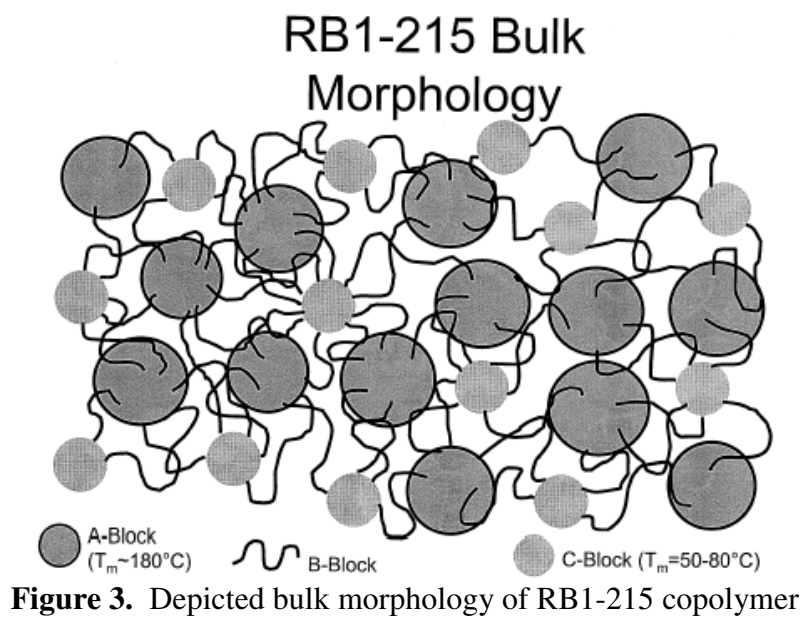
Figure 2. Stirred tank reactor systems (45-psig pressurized 1-L glass reactor on left and 4,500 psig Parr reactor systems on the right) that are available for this work.

Figure 3. Depicted bulk morphology of RB1-215 copolymer

2.2 Postprocessing

After the polymerization runs, the RB1-215 polymer product was separated from the reactor solvents , unreacted monomers, and unreacted initiator. First, the polymer was coagulated with excess water (3:1 v/v or more) out of the reactor fluid into a gel or dough (Figure 4 below).

Figure 4. Coagulated RB1-215 product on a Petri dish

Then, solvent and unreacted reactants are extracted from the dough. The dough is dried into a purified and safe-to-handle product, and melt-blended with other components, if needed (Figure 5 below).

2.3 Solvent/Reactant Extraction

The residual solvent and reactants must be removed from the "dough". Initial attempts to purify the polymer included one vacuum oven drying step (4 hours at 80 $^{\circ}$C), used to drive off the residual solvent, and followed by up to three supercritical CO$_2$ extraction steps (8 hour soak at room temperature and 2000 psig), used to remove unreacted monomers, oligomers and residual solvent.

Figure 5. Dried and melt-blended RB1-215 product on a Petri dish

2.4 Membrane-related Foaming Experiments

Figure 6 below depicts the preliminary testing procedure used to screen various polymers for gas sorption and diffusion, which translates to permeabilities. The polymer sheet of 1.61-2.34 mm in thickness (L_0) is exposed to the gas (CO_2 or N_2) at constant temperature and pressure for a certain period of time. Then, the pressure is adiabatically reduced to atmospheric for 1 minute or less. A portion of the sample adjacent to the surface will form a foam, while the interior will be unfoamed. This unfoamed region will have a thickness of L_u. Thus, the penetration distance, ΔL, of the gas will be

$$\Delta L = \frac{L_0 - L_u}{2} \qquad\qquad (8).$$

Expose at constant T, P, for a period of time

Then, freeze-fracture to show Penetration Depth, ΔL

Foamed Portion

Unfoamed Portion

L_0

L_u

Penetration Depth, $\Delta L = (L_0 - L_u)/2$
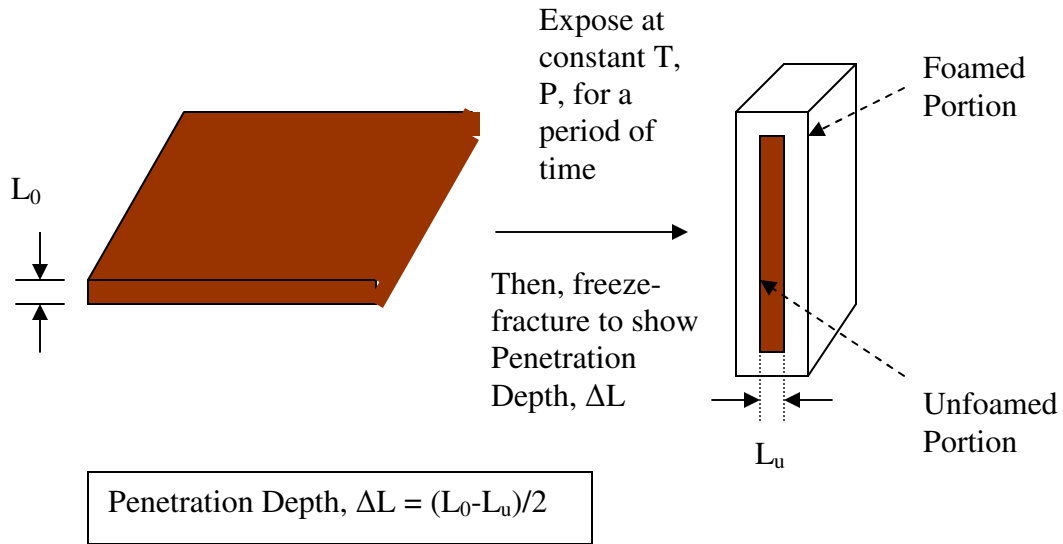
Figure 6. Procedure used to determine the penetration depth of a gas into the polymer.

Figure 7 below shows some of the details of the apparatus used by this project to generate monolithic polymer foams in order to gauge their capabilities of absorbing CO$_2$ and N$_2$.

(a)

(b)

Figure 7. Apparatus used to produce foam layers onto polymer samples: (a) is the cell used to contain the polymer; and, (b) is the syringe pump and piping system used to meter liquid carbon dioxide into the pressure cell where it turned into a gas or a supercritical fluid.

3. RESULTS

3.1 Fractional Precipitation

The polymer RB1-222 (similar to RB1-215) was fractionated with 50% ethanol/water solution. The polymer solution was diluted either 10:1 or 5:1 v/v with NMP as solvent. Based on the fractogram (Figure 8), there is very little intermediate Stage 1 precipitate (Block A product) at 0-15 ml precipitant added. A quantitative analysis of indicates that the unreacted Stage 1 contamination amounts to less than 1 wt% of the product copolymer. This result of relatively insignificant unreacted Stage 1 contamination seems to be generally the case.
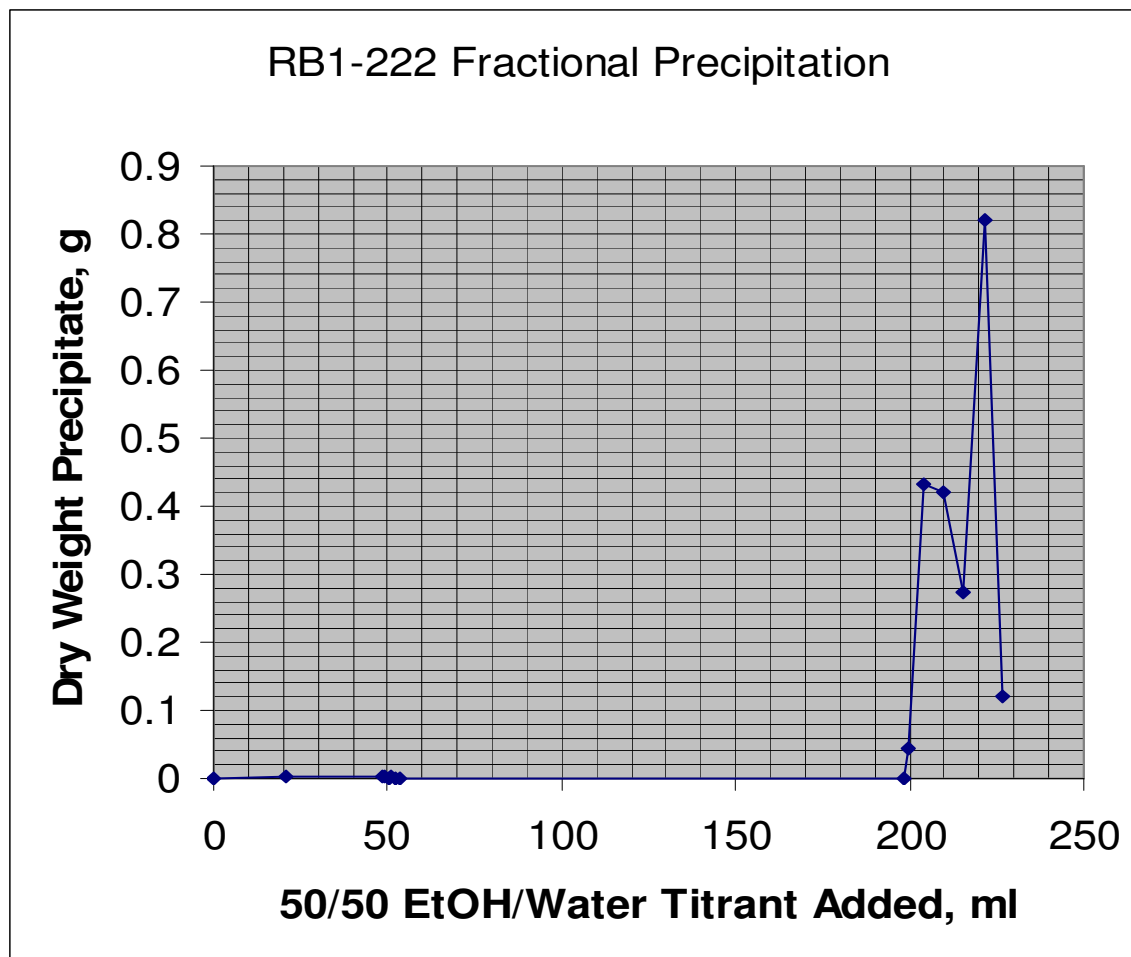
Figure 8. Fractional precipitation data for RB1-222 (similar to RB1-215) copolymer product

3.2 Foam Formation

Results of the foaming experiment depicted in Figure 6 are shown in Table 3 below.

Table 3. Results of 1-hr gas penetration experiments in various polymers.

Polymer	T, °C	P, psig	L$_0$, mm	L$_u$, mm	ΔL, mm
PMMA	47-48	700-750 CO$_2$	1.65	1.65	~0
PVMK	47-48	700-750 CO$_2$	2.34	1.48	0.43
RB1-215	47-48	930-933 CO$_2$	1.905	~0	~1.905
RB1-217 (Similar to RB1-215)	36	740-750 CO$_2$	1.615	~0	~1.615
RB1-215	36	1500 N$_2$	1.905	~1.905	~0
RB1-217	36	1500 N$_2$	1.615	~1.615	~0

Some of the fractured surfaces are shown in Figures 9-12 below.
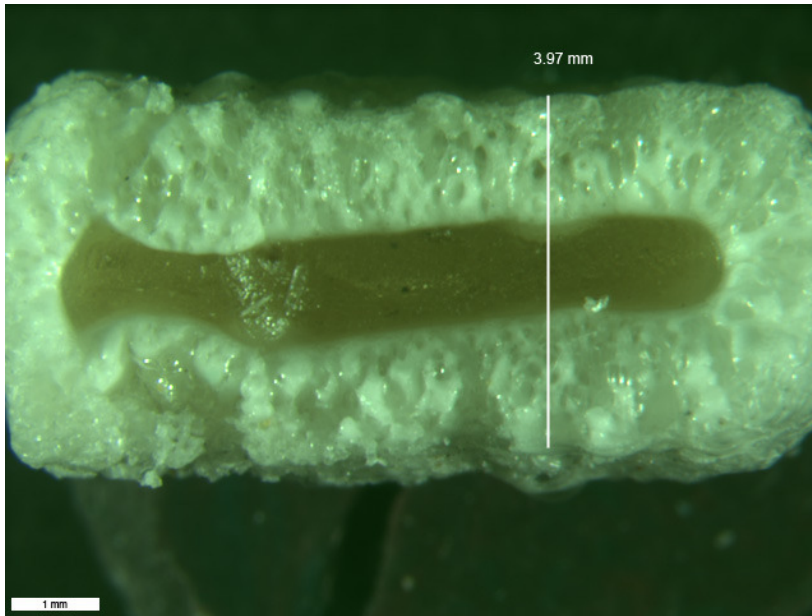
Figure 9. Foamed and unfoamed interior portion of a poly(vinyl methyl ketone) (PVMK) sample, showing the unfoamed region to be 1.48 mm thick.
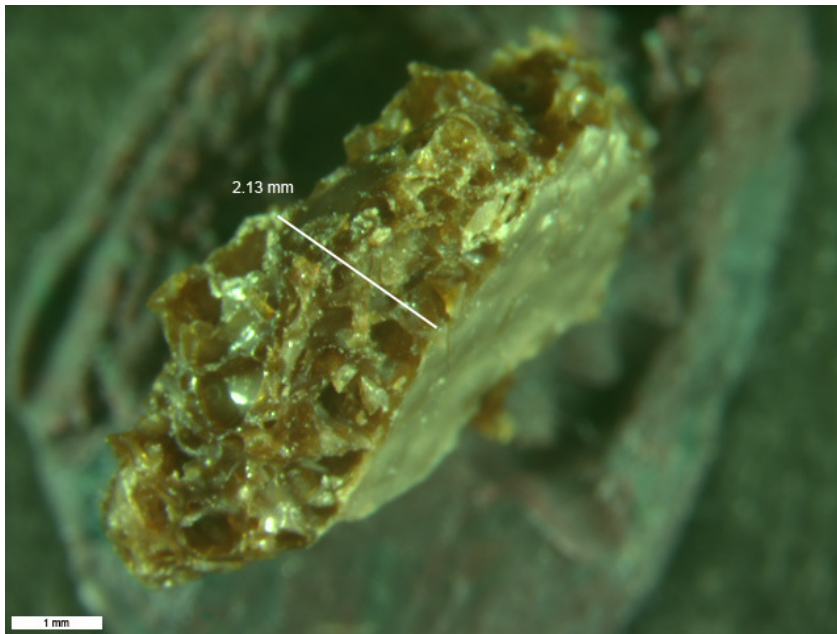

Figure 10. Foamed and unfoamed interior portion of an RB1-217 sample (similar to RB1-215), showing the unfoamed region to be almost nonexistent.
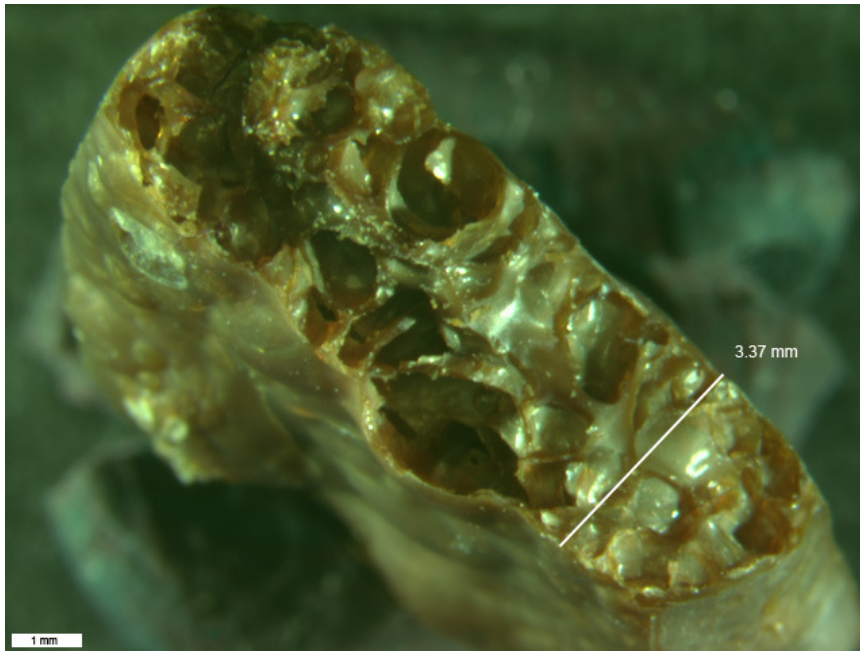
Figure 11. Foamed and unfoamed interior portion of an RB1-215 sample, showing the unfoamed region to be almost nonexistent.
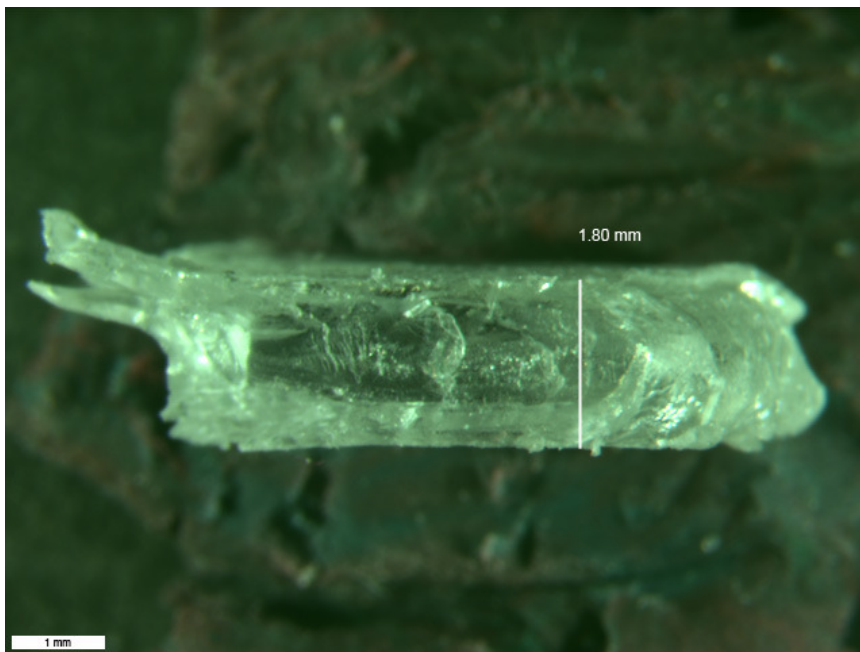

Figure 12. Foamed and unfoamed interior portion of a PMMA sample, showing the almost no foamed region.

3.3 DSC/TGA Analysis

Results of thermal analyses that were done with intermediate and final products agree with the thermal transitions depicted in Figure 3.

4. DISCUSSION OF RESULTS

From Table 3 and Figures 9-12, it is evident that the RB1-215 material has promise as CO_2 separation membranes from N_2. This is seen from the zero penetration depth for N_2 compared to CO_2 even at N_2 pressure of 1500 psig, compared to 750 psig for CO_2. These relative penetration depth values also indicate large relative permeability values of CO_2 to N_2 for the RB1-215-type of polymer.

It is possible to determine an order-of-magnitude estimate of the minimum CO_2 diffusivity for the RB1-217 membrane through the following equation

$$\frac{Dt}{(\Delta L)^2} \approx 1$$
$$D \approx \frac{(\Delta L)^2}{t} \tag{9}$$

Thus, for the penetration thickness of 1.614 mm and exposure time of 1 hr or 3600 s, the diffusivity is at least 7.2×10^{-6} cm^2/s, which is a relatively large number for diffusion of penetrants in polymer materials.

Thus, it is evident that the RB1-215-type material has been developed to be a promising membrane for continuous separation of CO_2 from N_2.

5. CONCLUSION

The development of multifunctional block copolymers has therefore been shown to possibly result in the development of CO_2-separating membranes for carbon sequestration applications.

ACKNOWLEDGEMENTS

REFERENCES

1. Crank, J., **1970**, "Mathematics of Diffusion", Oxford University Press, London.
2. McCabe, W.L, Smith, J.C., and Harriott, P., "Unit Operations of Chemical Engineering", 7th Edition, McGraw-Hill Book Co, 2005, Chapter 26.
3. Robinson, C., **1950**, *Proc. R. Soc.*, A204, 339.
4. Crank, J. and Robinson, C., **1951**, *Proc. R. Soc.*, A204, 549
5. Hutcheon, A.T., Kokes, R.J., Hoard, J.L., and Long, F.A., **1952**, *J. Chem. Phys.*, 20, 1232.
6. Bueche, F., Cashin, W.M., and Debye, P.V., **1952**, *J. Chem. Phys.*, 20, 1956
7. Bressler, S.E., Zakharov, G.M., and Kirrilov, S.V., **1961**, *Vysokomolek. Seodin.*, 3, 1072
8. Moore, R.S. and Ferry, J.D., **1962**, *J. Phys. Chem., Wash.*, 66, 2699
9. Auerbach, I. And Gehman, S.D., **1954**, *Analyt. Chem.*, 26, 658
10. Gillespie, T. and Williams, B.M., **1966**, *J. Polym. Sci. A-1*, 4, 933
11. Gosting, L.J., **1956**, *Adv. Protein Chem.*, 11, 429
12. Matano, C., **1932-3**, *Jap. J. Phys.*, 8, 109
13. Caneba, G.T., "Free-Radical Retrograde-Precipitation Polymerization Process," U.S. Patent No. 5,173,551, December 22, **1992**
14. Caneba, G.T., "Formation of Radicalized Vinylidene Chloride Copolymer Particulates and Related Materials", provisional U.S. patent application, June, **2007**